

Towards predicting neoplastic recurrence with multi-parametric MR

E. I. Zacharaki¹, R. Verma¹, S. Chawla¹, E. R. Melhem¹, R. Wolf¹, and C. Davatzikos¹

¹Department of Radiology, University of Pennsylvania, Philadelphia, PA, United States

Introduction: Treatment of brain neoplasms can greatly benefit from knowledge of the extent and degree of neoplastic infiltration. The true boundary of many neoplasms is difficult to identify with conventional approaches, especially in gliomas which are diffuse and infiltrative. Depending on location, large portions of brain neoplasms may remain untreated or sub-optimally treated such that time to recurrence shortens and prognosis worsens. While individual MR modalities provide information about some aspects of the neoplasm [1], no single modality is capable of providing a comprehensive tissue characterization. Properly combining such diverse MR protocols is likely to enhance discriminatory power and specificity, and to better highlight the extent and degree of neoplastic infiltration responsible for the post-treatment recurrence. While MRI-based methods for tumor segmentation [2,3] and neoplastic or healthy tissue characterization [4] have been investigated, little has been done to identify the likelihood of recurrence in the tissue surrounding the neoplasm, based on multi-parametric imaging. On the other hand, studies such as in [5], identify global variables (such as the presence of diffuse tumor margin) associated with incomplete resection and increased rate of recurrence, but they do not assess local tissue characteristics that could potentially aid adapting the therapy planning to treat some areas more intensely than others. The current work incorporates high dimensional intensity features created from multiple MRI acquisition protocols (structural MRI as well as DTI) into a pattern classification framework, to obtain a voxel-wise probabilistic spatial map that reflects the likelihood of a region presenting neoplastic recurrence after treatment. This is a preliminary study aiming to illustrate how the integration of multiple MRI parameters via sophisticated nonlinear pattern classification methods could be applied to predict possible neoplastic progression.

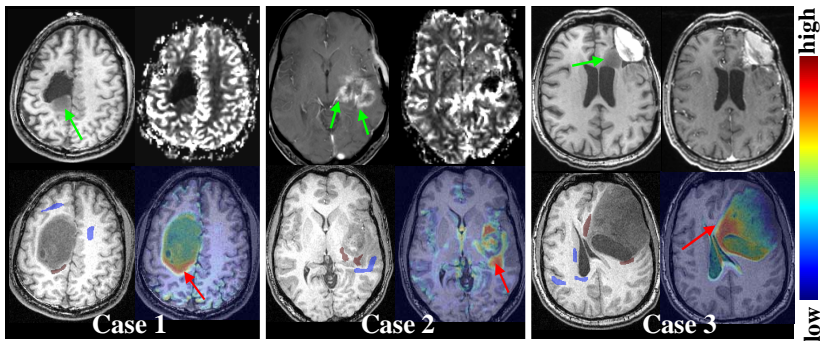


Fig. 1. Maps of tumor recurrence using *inter-patient* classifiers. For each case 1-3, the *top row* shows some post-resection scans; arrows point to regions identified as possible recurrence. *Bottom row, left:* Pre-resection scans showing the regions used for training: blue for healthy tissue, burgundy for recurrence in follow-up scans. *Bottom row, right:* Maps of likelihood of tumor recurrence with red indicating higher degree of abnormality. Red arrows are used to indicate regions in which recurrence actually occurred in follow-up scans.

Methods: The tissue profile for each patient is composed of 6 co-registered MR modalities, including 4 structural images, namely, B0, Fluid-Attenuated Inversion Recovery (FLAIR), T1-weighted, and gadolinium-enhanced T1-weighted (GAD), and two scalar maps computed from the DTI, namely, Fractional Anisotropy (FA) and Apparent Diffusion Coefficient (ADC). The datasets consist of longitudinal scans, across several time points, before and after surgery. The patients showed no evidence for residual enhancing tumor after surgery; however, the neoplasms recurred a few months later at or near the site of initial resection. Recurrence was confirmed by advanced imaging (e.g. perfusion) and a second craniotomy. These cases are representative for developing abnormality over time possibly due to neoplastic infiltration. Currently, we have only 3 datasets with all the required imaging modalities and a history report as described. These cases were diagnosed as anaplastic oligodendroglioma, glioblastoma and malignant meningioma, and are shown in Fig.1 from left to right, respectively. The regions of recurrence were identified by an expert by considering MR modalities in the follow-up images. Fig. 1 (top row) shows slices from some post-resection scans. Hypointensity in T1 images (cases 1, 3), increased enhancement in GAD (cases 2, 3) and high rCBV computed from perfusion images (case 2), indicate regions of high risk (pointed out by green arrows).

These regions are outside the visible resection boundary. Thus, their location can be estimated in the pre-resection scans. The determination of the position of these probable recurrence regions in the pre-resection scans was performed in an approximate fashion, based on visual cues from the anatomical images and guided by the result of elastic registration of the post-resection to the pre-resection images, accounting for tissue deformation caused by resection. These regions (marked in burgundy in Fig.1, bottom left) were used as samples for voxels with high likelihood for neoplastic progression. Samples for the healthy class (depicted in blue) were delineated close to the neoplasm, as well as away from it, in order to sample the variability fully. The samples for the two classes were used to train an SVM (Support Vector Machine) [6] classifier. For each sample (voxel), intensity values from each of the modalities are combined into a feature vector that serves as this voxel's appearance signature. In order to render this feature vector more robust to noise, we incorporated neighborhood information and stacked the 6-dimensional intensity features for each neighboring voxel into a long feature vector. At each instance of training, one patient was left out. Then the classifier, applied to this left-out patient, produced voxel-wise SVM pseudo-probability scores. These scores comprise a *recurrence probability map* that is indicative of the voxel-wise likelihood of recurrence.

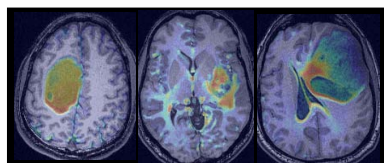


Fig. 2. Maps of tumor recurrence using *intra-patient* classifiers.

Results: The preprocessing of the images was performed with the public software package FSL and involved noise reduction and co-registration of all modalities to the T1-weighted image space. Data was made comparable across patients by applying histogram matching of the intensities. The recurrence probability maps for the 3 cases under study are shown in Fig.1, bottom row, on the right. The results are assessed by comparing the predicted areas of high probability (reddish areas on the right) with the regions that actually recurred (burgundy regions on the left). For the purposes of comparison, we constructed also an intra-patient classifier (Fig.2). Such a classifier is trained using samples from the patient to be evaluated. Although an intra-patient classifier requires retrospective knowledge of the recurrence and is therefore not applicable, it is useful (i) for assessing the ability of the classifier to reproduce the ground truth and (ii) for illustrating the performance without the inter-patient variability. It can be noticed that both classifiers are able to detect the suspicious regions with the inter-patient classifier being more specific. Moreover, the high similarity between

the probability maps calculated with the inter- and intra-patient classifiers demonstrates the generalization ability of the inter-patient classification scheme, which is the only one that can be applied for evaluation of neoplastic progression of new coming patients.

Discussion: We presented a framework for characterizing the imaging profile of abnormal tissue that transformed to a neoplasm. Although we used a small dataset for the identification of regions of high tumor recurrence probability, the quantification of the degree of abnormality by the probability maps in this manner illustrates the concept of anticipating sites of recurrence requiring more aggressive or alternate therapies. Also, though there could have been inaccuracies in identifying the regions of recurrence for training the classifier, we were able to demonstrate that these regions were in accordance with the regions predicted to have high probability of recurrence. Future studies are necessary to provide a more extensive training basis for the classifiers to detect progression and recurrence, and to further validate the performance of this computer analysis methodology.

References:

- 1) Young RJ, Knopp EA. *Journal of Magnetic Resonance Imaging*; 24(4): 709-724, 2006.
- 2) Prastawa M, et al. *Medical Image Analysis*; 8(3): 275-283, 2004.
- 3) Kaus MR, et al. *Radiology*; 218(2): 586-591, 2001.
- 4) Ou Y, et al. *Proceedings of ISMRM 2007*, Prog. 619, pp.137.
- 5) Talos I-F, et al. *Radiology*; 239(2): 506-513, 2006.
- 6) Collobert R, et al. *Journal of Machine Learning Research*; 1:143-160, 2001.